Numerical investigations on flow boiling heat transfer of ammonia water binary solution (NH3/H2O) in a horizontal microchannel

Yang, Ren; Wang, Yi; Li, Yongliang

DOI:
10.1016/j.ijheatmasstransfer.2021.121091

Numerical investigations on flow boiling heat transfer of ammonia water binary solution (NH_3/H_2O) in a horizontal microchannel

Ren Yang, Yi Wang*, Yongliang Li*

School of Chemical Engineering, University of Birmingham, Edgbaston, Birmingham B15 2TT, United Kingdom

*Corresponding authors: Y.Wang.23@bham.ac.uk (Y. W) and y.li.1@bham.ac.uk (Y. L)

Abstract

The flow boiling heat transfer characteristics of NH_3/H_2O mixture in a 2D single horizontal microchannel (0.4 mm width × 6 mm length) was investigated by Computational Fluid Dynamics (CFD) method. The multiphase VOF model and modified phase change Lee method were adopted to address the non-isothermal phase change process of the flowing zeotropic NH_3/H_2O mixture, while the variations of the binary mixture thermophysical properties were also taken into account. The effects of mass flux (46~552 kg/(m^2·K)), inlet NH_3 concentration (0-35% by mole) and heating wall temperature (20.5~70 ˚C) on the overall and local flow boiling heat transfer performance have been comparatively evaluated under constant heating wall temperature. According to the numerical results, the heat dissipation rate of NH_3/H_2O mixture flow boiling could reach up to 1.41 MW/m^2 at a mass flux of 552 kg/(m^2·s), which was 2.05 times of water single-phase flow cooling under the same constant heating wall temperature of 50 ˚C. It was also revealed that, for NH_3/H_2O mixture flow boiling in the microchannel, there was a threshold of inlet NH_3 concentration to maintain a certain level of heat dissipation rate at a given mass flow rate and further increasing the inlet NH_3 concentration would no longer benefit the amount of heat being dissipated. Furthermore, there were no local dry-outs found throughout the whole microchannel length under all the simulation conditions in this study, which could be attributed to the unique flow boiling behaviors of zeotropic NH_3/H_2O mixture. Therefore, it can be noticed that NH_3/H_2O mixture is a good alternative coolant for preventing local dry-outs and maintaining a certain functional temperature of electronic components.

Keywords: flow boiling heat transfer, microchannel, zeotropic NH_3/H_2O mixture, numerical simulation

1 Introduction

As the electronic components keep going smaller and their power densities continuously shoot higher, flow boiling in microchannels has been widely recognized as one of the more promising and efficient cooling methods due to its advantages such as large heat transfer area to volume ratio, small temperature variation on heated surface and high heat transfer performance with small amount of required coolant mass flux [1]. Zeotropic mixtures have been considered as alternative refrigerants replacing pure fluids in certain applications to improve the overall energy efficiency of power-generation and refrigeration systems. Especially in phase change-related thermal applications, the heat transfer irreversibility in heat exchangers could be reduced significantly due to the temperature glide in non-isothermal phase change processes of zeotropic mixtures at a constant pressure. Wang et al. [2] experimentally investigated the zeotropic mixture effect on the low-temperature solar Rankine cycle performance and found that the overall cycle efficiency of R245fa/R152a (0.7/0.3 by mass) mixture was 45.5% higher compared with that of pure R245fa. Zheng et al. [3] also discovered that the R161/R600a (0.25/0.75 by mass) mixture could enhance the system efficiency of a solar energy-powered refrigeration cycle by 39.6% and 54.7% comparing with pure R600a and R161, respectively. Furthermore, the thermophysical properties of zeotropic mixtures at a given pressure (e.g. saturation temperature) could be flexibly adjusted by tuning the inlet concentration of the more volatile component. Thus, they are advantageous in multi-phase related thermal managements where there are restrict limits for the maximum device/system temperatures ensuring sustainable operations, such as in high power electronics industries. For example, water cannot be boiled at 50 ˚C and 1 bar pressure but NH_3/H_2O mixture can if an appropriate NH_3 concentration is chosen. Marcinichen et al. [4] pointed out that the temperature of microprocessor chips should be kept below 85 ˚C with small temperature nonuniformity in order to achieve satisfactory calculating performance while maintaining high levels of reliability and safety. Leão et al. [5] conducted experimental investigations on flow boiling heat transfer of R32/R125/R134a mixture (23/25/52 by weight) at saturation temperature of 25 ˚C in multi-channel rectangular heat sink for thermal management of high-power density electronic components, and found that the maximally achieved average heat transfer coefficient (HTC) could be up to 30 kW/(m^2·K).

Accordingly, experimental studies on flow boiling heat transfer of zeotropic mixtures in mini/micro-channels have been conducted in literature. Guo et al. [6] investigated flow boiling heat transfer performance of R134a/R245fa (0.82/0.18 by mass) mixture in a horizontal tube with inner diameter of 3 mm and found that the binary mixture had less pressure drop and higher HTC than that of pure R245fa. Dang et al. [7, 8] carried out experimental studies on flow boiling heat transfer characteristics of R134a/R245fa mixture in a single rectangular microchannel (1mm×1mm) and a seven-parallel segmented microchannel (2mm×1mm) at constant saturated temperatures of 18.5 and 26 ˚C. They discovered that the flow boiling HTC of zeotropic mixtures in mini-channels were typically lower than the original pure fluids in most conditions, but the mixtures could delay surface dry-outs at high heat fluxes and also increase the critical heat flux (CHF) values significantly compared with pure fluids. Azzolin et al. [9] and In et al. [10] noticed that flow boiling HTCs of R1234ze(E)/R32 mixture and R123/R134a mixtures in microchannels with diameters of 0.96 mm and 0.19 mm were smaller than those of corresponding pure fluids at most experimental conditions, respectively. Results showed that the zeotropic mixture had higher CHFs than pure R134a though smaller HTCs at most cases. Five flow pattern regimes including the bubbly, confined bubbly, slug, churn-annular and annular flow were observed and the transitions among different regimes for binary mixtures were delayed comparing with pure fluids. It was suggested that the hysteresis, directly influenced by the inlet concentration of the more volatile component, considerably affects the overall flow boiling heat transfer performance.

Besides experimental efforts, computational fluid dynamic (CFD) simulation has also been adopted as an effective approach for describing multiphase flow heat transfer in microchannels since it could provide visualized transient spatial and temporal distributions (e.g. temperature and flow patterns) in complex flow and heat transfer processes, which cannot be accomplished through experiments. However, most of those relevant numerical studies in literature [11] have been mainly focused on multiphase flow and heat transfer processes of pure fluids such as water and other pure refrigerants. It is clear that, comparing to pure fluids, multiphase flow behaviors of miscible zeotropic mixtures are much more complex. Especially, the liquid/gas interface of miscible fluids under phase transitions changes depending on many factors (e.g. the varying concentration of the more volatile component in the bulk fluid) and difficult to be captured by regular mathematical descriptions. It is commonly known that the volume of fluid (VOF) method is capable of simulating immiscible mixture by tracking separated volume fraction of fluids [12]. However, in order to simulate flow boiling heat transfer of binary mixtures, the VOF model has been modified with reasonable assumptions in literature. For example, by coupling the effective diffusion model of liquid mixture with VOF method, Banerjee [13] investigated mass and heat transfer process between ethanol/isooctane mixture and air in a 2D macro-scale countercurrent stratified flow domain in ANSYS Fluent. Using the same methods, Zhang et al. [14] studied flow boiling heat transfer of isobutene/pentane mixture in a 2D countercurrent flow domain with inner diameter of 4 mm and outer diameter of 10 mm. Additionally, considering the vapor and liquid solutions as uniform mixtures, Lima et al. [15] studied the steady heat and mass transfer of NH_3/H_2O mixture flowing in a 2D macro-scale plate absorber using ANSYS CFX software.

NH_3/H_2O mixture has been a useful working fluid in large industrial refrigeration systems for decades. One advantage of NH_3/H_2O mixture is its high latent heat of evaporation. The latent heat of evaporation of NH_3/H_2O, R134a/R245fa, and R123/R134a mixture (0.2/0.8 by mass) at saturated temperature of 323.15 K are 1689 kJ/kg, 167 kJ/kg and 155.5 kJ/kg, respectively (calculated by REFPROP). Kærn et al. [16] systematically evaluated existing flow boiling heat transfer correlations for the macro-scale NH_3/H_2O mixture heat exchanger design, including two NH_3/H_2O flow boiling correlations and three flow boiling heat transfer correlations modified based on pool boiling correlations. Khir et al. [17] investigated flow boiling heat transfer of NH_3/H_2O mixture in a vertical tube with inner diameter of 6 mm and validated Mishra's model [18] with a new set of correlations. Furthermore, there have also been experimental studies specifically on flow boiling heat transfer of NH_3/H_2O mixture in mini-scale channels. Taboas et al. [19, 20] studied flow boiling heat transfer of NH_3/H_2O mixture in a vertical plate heat exchanger with hydraulic diameter of 4 mm. It was revealed that the flow boiling HTC of NH_3/H_2O mixture was highly dependent on mass flux but negligibly affected by heat flux and pressure at high vapor quality from 0.1 to 0.22. Arima et al. [21, 22] looked into flow boiling heat transfer of NH_3/H_2O mixture in a vertical plate evaporator with a gap size of 2 mm. It was found that the local HTCs increased with the increasing of mass flux but decreased with heat flux at certain experimental conditions. Bor et al. [23] showed that the HTC of NH_3/H_2O in a single channel annulus (hydraulic diameter of 0.4 mm and length of 0.8 m) was increased with inlet vapor quality, mass flux and heat flux. However, it can be noticed that most of those experimental studies were conducted in heat exchangers with large tube sizes and those related empirical correlations will not be applicable in predicting flow boiling heat transfer performance of NH_3/H_2O in microchannels due to the differences in bubble dynamics and flow patterns [24]. In addition, few numerical studies of NH_3/H_2O flow boiling heat transfer in microchannels are available in literature. Hence, it is of great significance to conduct exclusive numerical studies towards flow boiling heat transfer characteristics of NH_3/H_2O mixture in microchannels.

As discussed, NH_3/H_2O (latent heat ~1689 kJ/kg) flow boiling in microchannels is a potential effective option for advanced thermal management of electronics cooling with maximum operating temperature of 85 ℃, which is a temperature lower than saturated temperature of water at atmospheric pressure. Therefore, in present work, numerical simulations were carried out to investigate the effects of inlet mass flux, inlet NH_3 concentration (by mole) and heating wall temperature on the overall and local heat transfer performance of NH_3/H_2O mixture in a single horizontal microchannel (0.4 mm width and 6 mm length) at constant wall temperature boundary condition. The effective thermophysical and transport properties of NH_3/H_2O mixture as well as modified phase change models (Lee model) were incorporated into VOF model (two fluid model) through UDFs in ANSYS Fluent.

2 Mathematical models

This study simulated the flow boiling heat transfer performance of NH_3/H_2O mixture in a 2-dimensional rectangular microchannel domain (0.4 mm width and 6.0 mm length) shown in Fig. 1(a). The non-uniform quadrilateral mesh was adopted for the entire computational domain displayed in Fig. 1(b), which was gradually refined towards the heating walls for capturing the small-size nucleating bubbles within the viscous boundary layers.

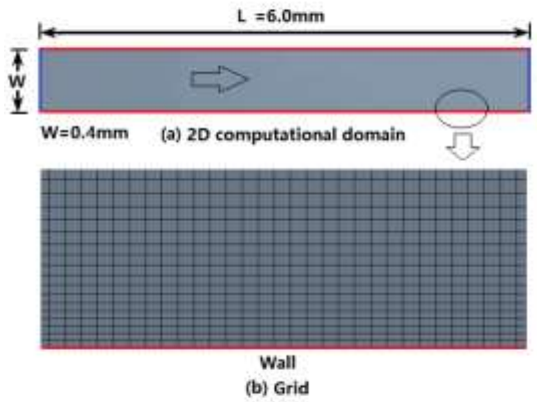

Fig. 1 Schematic of numerical simulation construction

The VOF model coupled with Lee method has been widely adopted to predict immiscible multiphase flow heat and mass transfer in mini/microchannels because of its robustness, time-saving and especially accuracy for mass conservation [11, 25]. In the present study, a transient VOF-explicit method and modified Lee model have been employed to track the liquid-gas interfaces of NH_3/H_2O mixture in flow boiling and characterize the mass and heat transfer associated with phase change. The NH_3/H_2O mixture at both liquid and gas state were assumed as a homogeneous saturated working fluid. In addition, it should be pointed out that the diffusion equations in the liquid and in the vapor phase are not directly considered in the present numerical simulation due to computational cost reasons and the lack of such appropriate diffusion equations, though remedies have been taken to better fit the numerical model for simulating the flow boiling of NH_3/H_2O mixture, including the use of effective thermophysical and transport properties of the mixture and modified Lee model in VOF model. The thermodynamic properties of NH_3/H_2O mixture (e.g. enthalpy) at vapor-liquid equilibrium were determined using correlations from Patek and Klomfar [26]. Other thermophysical properties of NH_3/H_2O mixture, including critical temperature and pressure, specific thermal capacity, thermal conductivity, dynamic viscosity, surface tension and density, were obtained by formulations proposed by Conde [27]. Furthermore, in the original Lee model, the mass transfer at liquid/gas interface is driven by the deviation of interfacial temperature from the saturation temperature of pure fluid, which is, apparently, not suitable for zeotropic mixture like NH_3/H_2O with more than one fluid components. It is generally accepted that the phase change phenomena of zeotropic NH_3/H_2O mixture are governed by the difference between local transient and saturated NH_3 concentration (a function of temperature and pressure) at the liquid/gas interface. Accordingly, a set of effective thermophysical properties of NH_3/H_2O mixture and modified Lee model were integrated in the simulation by UDF in ANSYS Fluent to fully describe the unique flow boiling behaviors of zeotropic NH_3/H_2O mixture.

Theoretically, when nucleation starts, a laminar single-phase flow will be disrupted due to the interactions between small bubbles and their neighboring liquids [28]. The realizable k-ε model was adopted due to its superior performance for complex flow and strong heat transfer, which has been seen and validated in previous investigations on flow boiling heat transfer in mini/microchannels from other researchers [29, 30]. The PISO algorithm was chosen for pressure-velocity coupling, the second-order upwind discretization for momentum and energy equations, as well as PRESTO and Geo-Reconstruct discretization for pressure and volume fraction interpolation, respectively. The variable time step was controlled by the Global Courant number up to 0.25 and the absolute residuals of the continuity equation was set to $1e^{-4}$.

2.1 VOF Method

In present work, the VOF method has been used to track the liquid-vapor interfaces in NH_3/H_2O mixture flow boiling by solving Navier-Stokes mass, momentum and energy conservation equations. The gravity effect was ignored for the 2-D computational domain. Also, Revellin et al. [31] found that gravity had little impact on flow boiling in microchannels when the channel size was less than 0.5 mm mainly due to the increased surface tension effect.

The continuity equation for each phase:

$$\frac{\partial}{\partial t}\left(\alpha_q \rho_q\right)+\nabla\cdot\left(\alpha_q \rho_q \vec{v}_q\right)=S_{m,pq} \tag{1}$$

$$\sum_{q=1}^{n}\alpha_q = 1 \tag{2}$$

where, α_q, ρ_q and $\vec{v}_q$ are the volume fraction, density and velocity of the q_{th} fluid in a grid, respectively. The sum of volume fractions equals to unity. $S_{m,pq}$ is the mass source term (kg/s) from the p_{th} phase to the q_{th} phase, which could be calculated by phase change model.

In this simulation, there are two phases including the liquid (p) and gas (q) phases in NH_3/H_2O mixture.

The momentum and energy equations:

$$\frac{\partial}{\partial t}\left(\rho\vec{v}\right)+\nabla\cdot\left(\rho\vec{v}\vec{v}\right)=-\nabla p+\nabla\cdot\left[\mu\left(\nabla\vec{v}+\nabla\vec{v}^{T}\right)\right]+\vec{F}_{surf} \tag{3}$$

$$\frac{\partial}{\partial t}\left(\rho E\right)+\nabla\cdot\left[\vec{v}\left(\rho E+p\right)\right]=\nabla\cdot\left(k_{\mathrm{eff}}\nabla T\right)+S_h \tag{4}$$

where, density ρ, dynamic viscosity μ and the effective thermal conductivity k_{eff} are all volume-averaged variables, while energy E and temperature T are mass-averaged values in a grid cell. S_h is the energy source term generated corresponding to the phase change process.

$$\rho=\sum_{q=1}^{n}\alpha_q\rho_q \tag{5}$$

$$E=\sum_{q=1}^{n}\alpha_q\rho_q E_q \Bigg/ \sum_{q=1}^{n}\alpha_q\rho_q \tag{6}$$

where, E_q is energy for each phase based on the specific heat of the q_{th} phase and the shared temperature value of two phases.

Surface tension force $\vec{F}_{surf}$ is considered as a source term in momentum equation, calculated by means of the continuum surface force method (CSF) as follows [32]:

$$\vec{F}_{surf}=\sigma\frac{\rho\kappa\nabla\alpha}{\left(\rho_p+\rho_q\right)/2} \tag{7}$$

where, κ is the local interface curvature and σ is the surface tension coefficient.

2.2 Phase change Model

Lee model is a simplified version of Schrage model, considering the quasi-thermo-equilibrium phase change existing at constant pressure condition and driven by the deviation of local temperature from the saturated temperature of the pure fluid [33]. As aforementioned, the evaporation of NH_3/H_2O mixture is a non-isothermal phase change process. Hence, the phase change phenomenon of NH_3/H_2O mixture is considered to be triggered by the difference between local transient and saturated NH_3 concentration of the liquid mixture (a function of local temperature and pressure) in each interfacial grid cell. Furthermore, the mass transfer rate at the liquid/gas interface should be proportional to the NH_3 concentration deviation. Therefore, the Lee model could be modified as follows:

$$\begin{cases} S_{m,pq} = -S_{m,qp} = -r_i \alpha_q \rho_q \left| \dfrac{x - x_{sat}}{x_{sat}} \right|, \quad x < x_{sat} \\ S_{m,pq} = -S_{m,qp} = +r_i \alpha_p \rho_p \left| \dfrac{x - x_{sat}}{x_{sat}} \right|, \quad x > x_{sat} \end{cases} \tag{8}$$

$$S_h = S_{m,pq} \cdot q_{LH} \tag{9}$$

where, q_{LH} is the latent heat of evaporation, x and x_{sat} are the local transient NH_3 concentration and the corresponding saturated concentration, the relaxation factor r_i is an empirical coefficient with the unit of s^{-1}, which is determined by factors such as mesh size, operational conditions and geometric parameters of heat sinks in specific cases [34, 35]. The value could be ranged from 0.1 to $1e^7$ s^{-1} for the least saturation temperature deviation in literature [11]. It was also pointed out that a small r_i value might cause the temperature in interfacial cells deviating from the saturation temperature, and a large value might increase the difficulty for the convergence of governing equations. In this study, 100 was selected for flow boiling heat and mass transfer simulation of NH_3/H_2O mixture, referring to previous related research [36, 37, 38, 39].

2.3 Initial and Boundary conditions

Considering the length of the computational domain is only 6 mm and the transient multiphase flow passes the channel in merely several milliseconds, the temperature of heating walls was set as a constant for this small dimensional and rapid process [13, 14, 40]. A velocity-inlet and pressure-outlet conditions were used in present simulation. To ensure fully developed flows at the channel outlet, the back-flow temperature was adjusted equal to the mass-averaged temperature of forward flow at the precious-step time (calculated by UDF) as follows:

$$T_{\text{backflow}} = \frac{\sum_{i=1}^{m} (\rho_i u_{xi} A_i \cdot T_i)}{\sum_{i=1}^{m} (\rho_i u_{xi} A_i)} ; u_{xi} > 0 \tag{10}$$

where, $T_{backflow}$ is the mass-averaged back-flow temperature and ρ_i, u_{xi}, A_i, T_i are the density, velocity in the x direction, area and temperature of mixture at the i_{th} grid cell of the outlet boundary, respectively.

Since the NH_3/H_2O mixture will be entering the channel at subcooling state, a steady single-phase flow field was simulated first and then the convergent results with residual of 10^{-5} were adopted as the initial condition for later flow boiling heat transfer simulation [41].

2.4 Mesh independence test and validation

A mesh independence test was conducted in the computational domain, shown in Figure 1. Eight mesh sizes were evaluated at mass flux of 46 kg/(m^2·s), NH_3 concentration of 30% and heating wall temperature of 50 ˚C.

The values of area-averaged vapor fraction on heating surfaces (i.e. x_{wall}) and heat flux at heating walls (i.e. q_{wall}) are plotted against varying grid size in Fig. 2 to demonstrate the grid size effect on the numerical results. It can be observed from the figure that when the average grid size was decreased to and below 6.2 μm, the variations of vapor fractions and heat fluxes among cases with different grid sizes were less than 3%. Therefore, an average grid size of 6.2 μm satisfactorily fulfilled the rule of mesh independence and was selected for the simulations in present study.

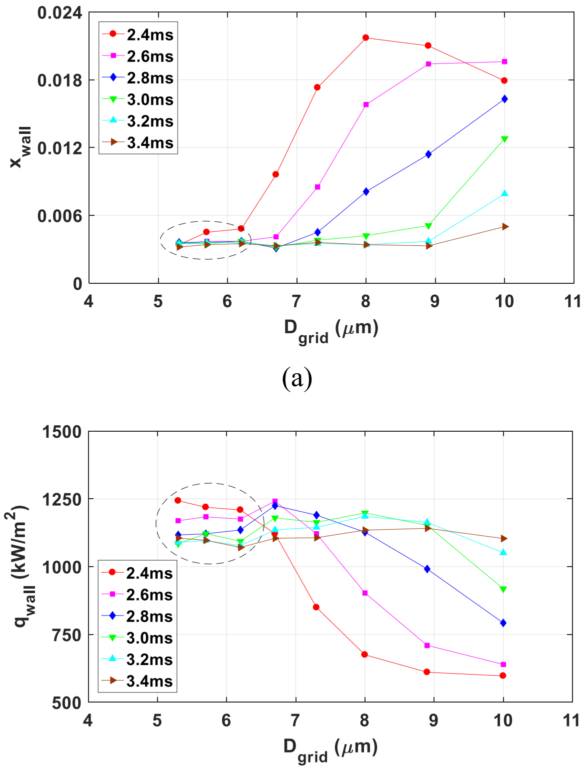

(a)

(b)

Fig. 2 Grid independent tests based on the vapor fraction (a) and heat flux (b) at the heating walls

Since few experimental studies of NH_3/H_2O mixture flow boiling in microchannels are available in literature and H_2O could be considered as a special NH_3/H_2O mixture with zero NH_3 concentration, the numerical construction in this study (e.g. VOF- original Lee model) was validated with experimental data of subcooled (T_{in}=30 ˚C) water flow boiling heat transfer in copper rectangular microchannels with similar hydraulic diameters [42, 43]. The contact angle of copper surface was chosen as 86˚ [44].

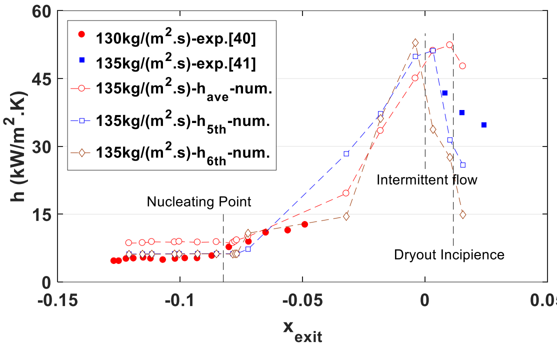

Fig. 3 Comparisons of HTC results among numerical and referenced experimental cases

The experimental results of overall HTC (h) versus exit vapor quality (x_{exit}) at various operating conditions as well as the HTC values calculated using the numerical set-up in this study were compared and are demonstrated in Fig. 3. The negative x_{exit} values were related to inlet subcooling conditions [45, 46]. In Fig. 3, the solid data points denote experimental results and the connected hollow-dots are for numerical results. h_{ave} is the average HTC of the whole computational domain, h_{5th} and h_{6th} are the average HTC values at channel axial locations of 4-5 mm and 5-6 mm, respectively. Fig. 3 indicates that the numerical results obtained based on the numerical system construction of this study are in good agreements with the experimental data within relative errors of ± 25%.

To further validate the VOF/modified LEE model in this study, additional numerical simulations were conducted based on a model of flow boiling heat transfer of R134a/R245fa mixture (70/30 by wt.%) in a 2D microchannel. The numerical conditions duplicated the experimental conditions in [47] such as the constant heat flux of 33 kW/m^2 and the evaporation temperature of 18.5℃. The thermodynamic & transport properties of R134a /R245fa binary mixture were obtained by using NIST REFPROP 9.1 [48]. The results of HTC and flow pattern comparisons between experimental and numerical cases are demonstrated in Fig. 4 and Fig. 5.

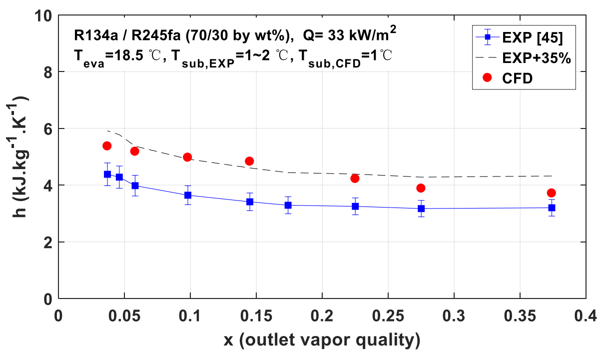

Fig.4 HTC result comparisons among numerical and referenced experimental cases of R134a/R245fa mixture (70/30 by wt.%) in the microchannel

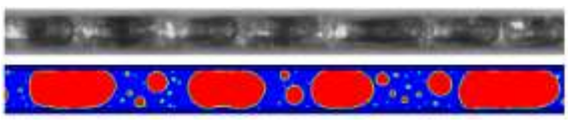

(a) Confined flow

(b) Slug flow

Fig.5 Comparisons of corresponding confined bubble and slug flow patterns of R134a/R245fa mixture (70/30 by wt.%) between the experiment and numerical simulation

As shown in Fig.4, the simulation results based on VOF - modified Lee model could well predict the tendency of HTC values as a function of channel outlet vapor quality under the constant heat flux conditions and the deviations of individual HTC values between experiment (blue points) and numerical simulation (red points) are within satisfactory expectations (35%). As the results indicated, the simulated values of HTC were over-predicted in comparison with the experimental data. One possible reason could be that mass diffusion equations were not considered in the present numerical model, which has been agreed as one of the main reasons that causes the heat transfer degradation of zeotropic mixture compared to pure fluids [47]. Ammonia water, as a zeotropic mixture, associates with more than two species (i.e. $NH_3{\cdot}H_2O$, NH_4^+, NH_2^-, OH^- and H_3O^+). Thus, the mass diffusion model exclusively for NH_3/H_2O mixture can be rarely found in literature. Furthermore, the computational cost would be too overwhelming even though such mass diffusion model exists. Alternatively, the mass transfer phenomena of different components in the NH_3/H_2O mixture has been taken into account by the use of effective thermophysical and transport properties of NH_3/H_2O mixture and modified phase change models (i.e. modified Lee model embedded in VOF model).

Further illustrated in Fig.5, the simulated flow patterns (e.g. confined bubble in Fig.5 (a) and slug flow in Fig.5 (b)) also match well with the corresponding experimentally visualized flow patterns of R134a/R245fa mixture (70/30 by wt.%) flow boiling in microchannel. Hence, the numerical system construction in this study (i.e. VOF - modified Lee model) has been validated and therefore can be properly used for the following investigations of NH_3/H_2O mixture flow boiling characteristics in the microchannel under the condition that there is almost no experimental data of NH_3/H_2O flow boiling in microchannels.

3 Results and discussion

In flow boiling research community, it is generally accepted that there are two main mechanisms (convection and nucleate boiling) for flow boiling heat transfer in microchannels. And the mass flux (dominates convection) and heat flux (related to wall superheat) are the most important factors affecting the flow boiling heat transfer performance [43, 51]. Furthermore, the inlet concentration of the more volatile component of a zeotropic mixture is one of the most distinctive parameters that differentiates flow boiling of zeotropic mixtures from pure fluids [7-10]. Therefore, as the numerical model was successfully validated in section 2.4, the effects of mass flux, inlet NH_3 concentration and heating surface temperature on flow boiling heat transfer of NH_3/H_2O mixture in microchannels were comprehensively investigated and compared under a constant wall temperature boundary condition. During the simulations, the heating wall temperature was set below 85 ˚C to comply with industrial standard of the maximum functional temperature of common micro-scale electronics [4, 49].

Accordingly, the relevant simulation conditions in this study are detailed in Table 1. Fig. 6 shows the phase diagram of NH_3/H_2O by mole fraction and temperature at 0.1 MPa, where the left line (blue) and the right line (red) is the saturated liquid and vapor line of NH_3, respectively. Based on the phase diagram, the mole fraction of NH_3 was selected from 0.2 to 0.36 to ensure the NH_3/H_2O mixture was at subcooled condition (T_{inlet}=20 ˚C) before entering the microchannel and underwent flow boiling under a wall temperature of 50 ˚C.

Table 1 Simulation conditions on flow boiling of NH_3/H_2O mixture

Parameter	Range
Mass flux (kg/(m^2·s))	46~552
NH_3 concentration (by mole)	0.15~ 0.35
Heating wall temperature (˚C)	20.5~70
Inlet fluid temperature (˚C)	20
Operational pressure (MPa)	0.1

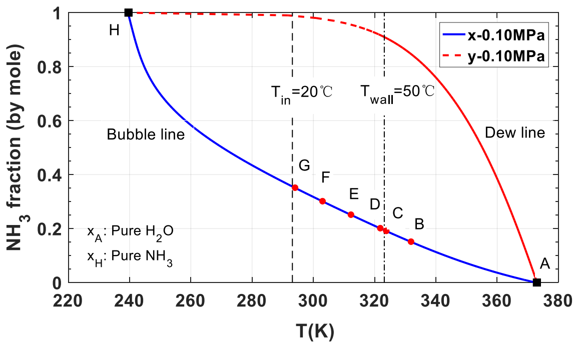

Fig. 6 Phase diagram of NH_3/H_2O mixture at 0.1 MPa

In addition, the microchannel heating surfaces were deliberately treated as superhydrophilic surfaces (zero contact angle) in this study featuring optimum flow boiling performance. In literature, it has been pointed out that superhydrophilic surface could considerably enhance flow boiling HTC and CHF in microchannels at high heat flux conditions mainly due to the uniform thin liquid film distribution on heating surface and the consequent delay to partial dryout [50, 51].

Both overall and local heat transfer performance of NH_3/H_2O mixture flowing through the microchannel were investigated. As mentioned earlier in Section 2, the transient arithmetic model was adopted in this simulation. However, the overall and local HTC results were obtained when the system reached dynamic equilibrium.

The overall HTC was calculated by

$$h_{\text{overall}} = \sum_{i=1}^{n}\left[\frac{\left(q_{\text{L,i}}+q_{\text{R,i}}\right)/2}{T_{\text{wall}}-(T_{in}+T_{\text{out,i}})/2}\right]\Bigg/n \tag{11}$$

where, $h_{overall}$ is the overall heat transfer coefficient (kW/(m^2·K)), q_L and q_R is the area-averaged heat flux (kW/m^2) at either the left and right heating wall of the 2-D microchannel, as shown in Fig. 7. T_{wall}, T_{in}

and T_{out} are the wall temperature (K), the inlet and outlet fluid temperature (K), respectively. The index "i" denotes an individual transient point in time after the dynamic equilibrium of flow boiling. A total number of "n" individual time points were considered for evaluating the time-average HTC within the equilibrium state.

The local heat transfer coefficient was calculated by

$$h_{\mathrm{local,j}} = \sum_{i=1,j}^{n} \left[\frac{\left(q_{\mathrm{l,j,i}} + q_{\mathrm{r,j,i}}\right)/2}{T_{\mathrm{wall}} - T_{\mathrm{fluid,j,i}}} \right] \bigg/ n \tag{12}$$

where, h_{local} is the local heat transfer coefficient (kW/(m^2·K)), q_l and q_r is the local area-averaged wall heat flux (kW/m^2) at either the left and right heating wall. The index "j" indicates the individual locations for where the local HTC being investigated, shown as "a1…a5" in Fig. 7. T_{fluid} is the local mass-averaged fluid temperature (K) corresponding to the individual locations "a1…a5". The length of each local area "a_j" is 0.5 mm.

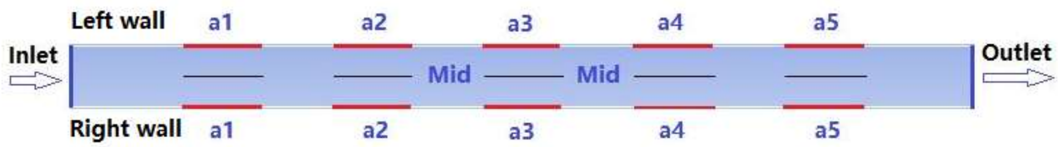

Fig. 7 Locations in microchannel domain for obtaining local parametric values

3.1 The effect of mass flux

The mass flux effect on subcooled flow boiling heat transfer of NH_3/H_2O mixture (x_{in}=0.35) at a constant heating wall temperature of 50 ˚C was investigated and compared with single-phase convective heat transfer of H_2O (x_{in}=0).

3.1.1 The overall heat transfer performance

The overall HTC of single-phase water convection and flow boiling of NH_3/H_2O are plotted against mass flux in Fig. 8.

As shown in Fig. 8(a), while the HTC of single-phase flow (green) is linearly correlated with varying mass flux, the HTC of NH_3/H_2O flow boiling (blue) firstly increases linearly with mass flux (A-B), followed by gradual decrease in growth rate (B-D) and eventually tended to be nearly constant with the further increase of mass flux (D-E). The corresponding flow patterns at A-E are illustrated in Fig. 8(b) as A, B are slug flow and D, E are bubbly flow. As the results show, the HTC vs. mass flux tendency of NH_3/H_2O is similar with the well-known flow boiling behavior, which features that HTC in nucleate boiling dominant region is depended upon heat flux but far less sensitive to mass flux and vapor quality, while it is dependent with mass flux and vapor quality but independent with heat flux in the convective boiling dominant region. Moreover, the nucleate boiling region is normally associated with low vapor quality that favor relatively small bubbles from nucleation, whereas the convective boiling region features high vapor quality flow pattern with nucleation inhibited [43, 52].

Moreover, it can be observed from Fig. 8(a) that the HTC values of NH_3/H_2O flow boiling are greater than those of single-phase water convection for all mass fluxes at 50 ˚C wall temperature. This means for a thermal application that has to operate below 50 ˚C, NH_3/H_2O (two phase) is a better choice than water (cannot boil at 50 ˚C at 0.1 MPa) in terms of heat transfer performance.

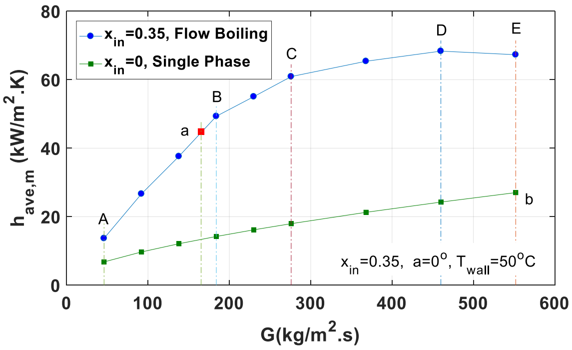

(a)

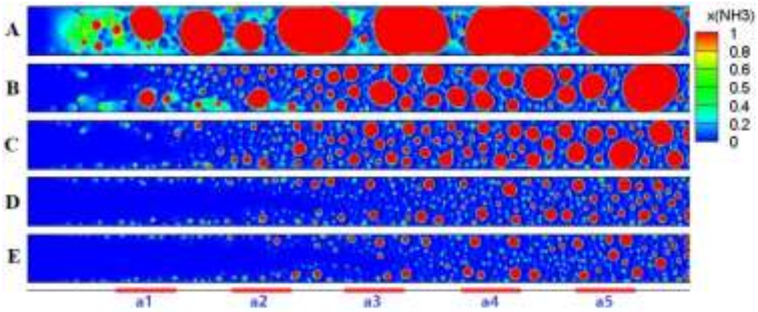

(b)

Fig. 8 The mass flux effect on overall HTC (a) and vapor fraction distribution (b) of NH_3/H_2O flow boiling in microchannel

To more completely evaluate the flow boiling heat transfer performance of NH_3/H_2O, in addition to the overall HTC results, the values of overall heat flux (average heat flux over the length of microchannel under constant wall temperature) are plotted as a function of mass flux in Fig. 9 to demonstrate the heat dissipation capability of NH_3/H_2O flow boiling in the microchannel.

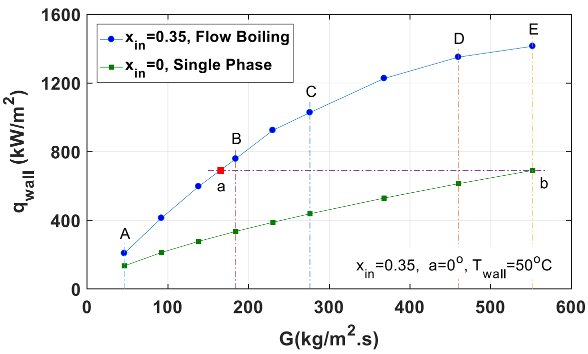

Fig. 9 The mass flux effect on overall heat flux of NH_3/H_2O in microchannel

As the figure shows, for the same mass flux of 552 kg/(m^2·s) at case point "E" and "b" in Fig. 9, the overall heat flux of NH_3/H_2O mixture flow boiling in a microchannel could reach up to 1.41 MW/m^2, which is 2.05 times the value of the single-phase H_2O convection (0.69 MW/m^2). Furthermore, for the same heat dissipation rate of 0.69 MW/m^2 at case point "a" and "b" in Fig. 9, to keep a constant device temperature (e.g. 50 ˚C), the required mass flux of NH_3/H_2O flow boiling is only 166.2 kg/(m^2·s), which is 30% the requirement of single-phase H_2O convection and therefore means less required pumping power supply. Hence, flow boiling heat transfer of NH_3/H_2O mixture in microchannels at least shows promises as an alternative thermal management method for high power density electronics though there are problems to be studied and solved in the future.

3.1.2 The local heat transfer performance

The local HTC and wall vapor fraction results of NH_3/H_2O flow boiling at various locations, shown as "a1-a5" in Fig. 7, within the microchannel are plotted in Fig. 10. As it can be noticed from Fig. 10(a), the HTC at "a1" that is close to the microchannel inlet, firstly increased from "A" to "F" and then decreased from "F" to "E" against mass flux. At low mass flux (A-F), increasing mass flux positively affected the local flow boiling heat transfer performance at "a1" by taking vapor bubbles away from the surface at a higher rate thereby benefiting local bubble growth. At high mass flux (F-E), local flow boiling at the inlet location "a1" was suppressed because there was not enough time for the fluid to interact with the hot surface and be fully boiled due to the high flow rate. Therefore, there was an optimum mass flux point at "F" where the two effects were best balanced. In addition, it can be observed from Fig. 10(a) that there existed a same maximum local HTC value for all locations (a1-a5) around 85 kW/(m^2·K) though occurring at different optimum mass fluxes. This shows the existence of a same upper limit for the effect of mutually benefiting nucleation and convection on local flow boiling performance, mainly governed by NH_3 concentration (i.e. the concentration of the more volatile component) under the constant heating wall temperature, regardless the location in microchannel.

However, the local flow boiling behavior near the microchannel outlet should be different from that at the inlet and that's why the HTC trends are different in Fig. 10(a) at different channel locations. This can be explained that the fluid just barely started to boil at the inlet and flow boiling was fully developed at the outlet as the fluid already went through the whole length of the heating surface. Another important situation to be noticed was that the NH_3 concentration in the bulk fluid, as the more volatile component, decreased along the channel (i.e. from "a1" to "a5"). Hence, at "a5" that is close to the microchannel outlet, the flow pattern was fully developed slug flow at low mass flux and fully developed bubbly flow at high mass flux under constant wall temperature condition (Fig. 8(b)) and more importantly there were limited amount of NH_3 left in the bulk fluid to be boiled. Accordingly, as shown in Fig. 10(a), the HTC value at "a5" grew with mass flux. As boiling was fully developed and little NH_3 left in the bulk fluid, the heat transfer performance was mainly dependent on the convective part and mass flux, which can be further supported by the near-zero wall vapor fraction of NH_3/H_2O, as shown in Fig. 10(b).

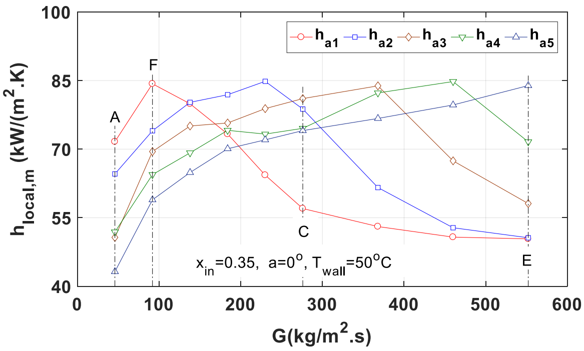

(a)

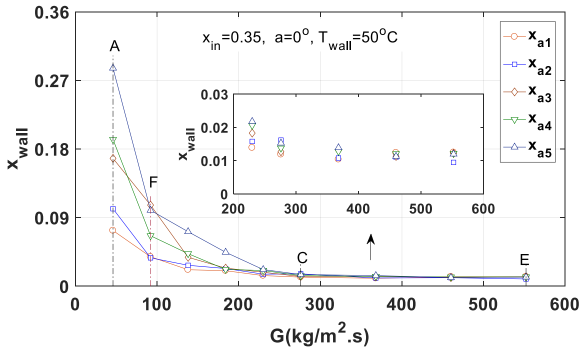

(b)

Fig. 10 The mass flux effect on local HTC (a) and vapor fraction at heating surfaces (b) of NH_3/H_2O flow boiling in microchannel

3.2 The effect of inlet NH_3 concentration

The concentration of the more volatile component, related to both thermal and mass diffusion, is the most essential factor governing the phase change heat transfer of binary mixtures. Therefore, the inlet concentration of NH_3 has to be carefully investigated especially that in this study the heated wall temperature was only above the saturation temperature of NH_3 not H_2O throughout the entire microchannel. Also, the degree of subcooling at a certain pressure is determined by the inlet concentration of NH_3, which will affect the temporal and spatial distributions of NH_3/H_2O flow boiling along the channel axis. Hence, the effect of inlet NH_3 concentration, including one single phase case (with x_{in}=0.19) and four subcooled flow boiling cases (with x_{in}=0.2, 0.25, 0.3 and 0.35), on heat transfer performance has been discussed below under a constant heating temperature of 50 ˚C and operational pressure of 0.1 MPa while the saturated concentration of NH_3/H_2O mixture is 0.194 at the corresponding conditions.

3.2.1 The overall heat transfer performance

Accordingly, the heat flux and HTC results of NH_3/H_2O mixture as a function of inlet NH_3 concentration are illustrated in Fig. 11. As it can be observed from Fig. 11(b), the average flow boiling HTCs at G=276 kg/(m^2·s) (brown line) were almost a constant when x_{in} of NH_3 < 0.2, which was so small that the effect of nucleate boiling was very limited. The overall HTCs were then increased with x_{in} because the effect of nucleate boiling came into play and got strengthened as x_{in} raised (e.g. c_0-c_1 in Fig. 11(b)) until the flow boiling characteristics within the channel reached a steady state as x_{in} was continuously increased. The reason might be that the increase of NH_3 concentration would not always be beneficial to the overall flow boiling performance as the effective number of nucleation sites might be reduced by the incremented number of vapor bubbles sitting on the heating surface. Also, the adverse effects on heat transfer from surface tension gradient and NH_3 dilution and dissolution induced by the NH_3 concentration gradient within the microchannel also have to be considered. Eventually, the HTCs almost got to the same value between two different x_{in} conditions, shown as c_1 and c_2 in the figure.

Furthermore, as indicated in the figure, the trends of HTC against x_{in} are different among various flow rates. The most important finding is that the HTC reached to a steady value earlier at smaller values of x_{in} for lower mass flow rate cases, which can be deduced through the comparison between the HTC curves of G=46 kg/(m^2·s) (red line) and G=276 kg/(m^2·s) (brown line). Flow rate is another factor besides inlet NH_3 concentration which affect the timing of the onset of nucleate boiling as well as the development of flow boiling stages within the length of the channel. As mentioned above, a faster fluid velocity means the fluid would have less time interacting with the heating channel surface which closely connects with triggering the boiling phenomena while the fluid would interact with the heating surface more for a lower fluid velocity. Similarly, the heat flux values dissipated from the heating wall to NH_3/H_2O mixture converged to constant values as the inlet NH_3 concentration incremented for different mass flow rate cases, as shown in Fig. 11(a) (e.g. red, blue line). The figure reveals that there is a threshold of inlet NH_3 concentration to maintain a certain level of heat dissipation rate at a given mass flow rate, for example, x_{in}=0.25 for G=184 kg/(m^2·s) (blue line). In addition, at x_{in}=0.25, it can be noticed that the wall heat flux value increased with the mass flux (Fig. 11(a)) as discussed earlier while the HTC did not follow the same principle, such as, with HTC at G=276 kg/(m^2·s) greater than that at G=552 kg/(m^2·s). The possible reason for this was that fluid temperature within the microchannel had to be considered besides heat flux when calculating the HTC and NH_3/H_2O mixture is a zeotropic mixture with non-isothermal phase change process.

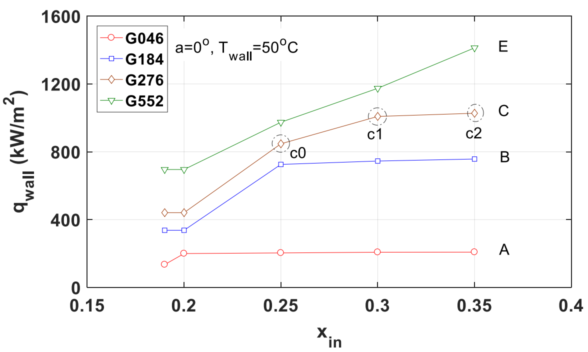

(a)

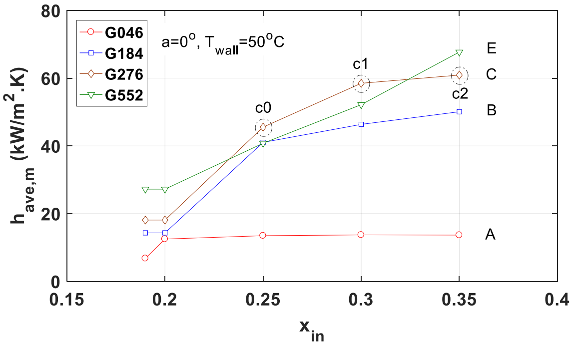

(b)

Fig. 11 The NH_3 concentration effect on overall heat flux (a) and HTC (b) of NH_3/H_2O flow boiling in microchannel

3.2.2 The local heat transfer performance

In addition, the effect of NH_3 inlet concentration on local flow boiling heat transfer characteristics was investigated. As illustrated in Fig. 12(a), at a fixed flow rate of 276 kg/(m^2·s), the HTC at "a1" (red line) linearly grew as the inlet concentration of NH_3 increased while the HTC at "a5" (blue line) first incremented to a maximum value before its decline. The explanation of this local HTC behavior is similar to the effect of NH_3 inlet concentration on overall flow boiling heat transfer performance. It was at early stage of nucleate boiling at "a1" near the channel inlet so that the added NH_3 concentration promoted the local bubble formation and nucleate boiling. On the other hand, boiling had already been developed for a long distance through the channel before arriving at "a5" where excessive and large vapor bubbles on the heating surface started suppressing boiling heat transfer at high NH_3 concentration. This could be further supported by the local flow patterns, shown in Fig. 12(b).

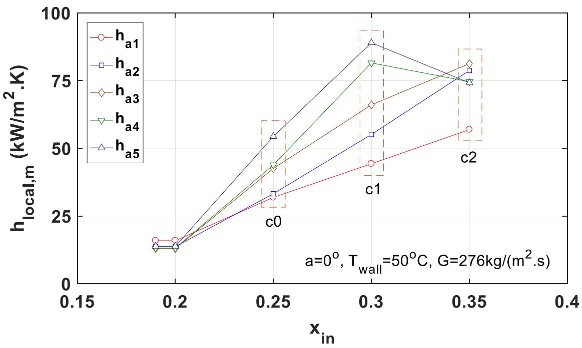

(a)

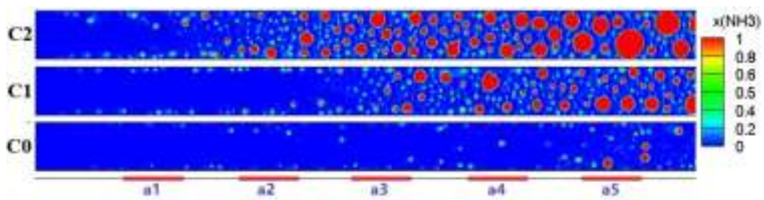

(b)

Fig. 12 The NH_3 concentration effect on local HTC (a) and vapor fraction distribution (b) of NH_3/H_2O flow boiling in microchannel

3.3 The effect of heating wall temperature

Previously, the mass flux and inlet NH_3 concentration effects on NH_3/H_2O mixture flow boiling heat transfer performance were investigated under the constant heating wall temperature of 50 ˚C. However, in practical applications related to this study, the functional temperature of most electronics would vary in a wider range that may be either lower or higher than 50 ˚C. Thus, the influence of heating wall temperature and mass flux on NH_3/H_2O mixture flow boiling heat transfer performance have been further discussed at a constant NH_3 inlet concentration of 0.35.

3.3.1 The overall heat transfer performance

In Fig. 13, the results of heat flux and HTC at different mass fluxes are plotted against heating wall temperature. As Fig. 13(a) shows, the overall heat flux of NH_3/H_2O mixture flow boiling heat transfer in the microchannel was linearly elevated as heating wall temperature increased due to the enhanced nucleate boiling. Also, the heat flux was larger at higher mass fluxes because of the enhancing effect of convection on the overall flow boiling heat transfer. Nevertheless, the trend of HTC, displayed in Fig. 13(b), was different from that of heat flux, in which the HTC did not linearly increase with heating wall temperature. The HTC value of NH_3/H_2O mixture flow boiling heat transfer was inherently connected with the flow patterns within the microchannel which was governed by the balance among heating wall temperature, NH_3 concentration and mass flux. As the heating wall temperature went higher, the HTC first increased linearly in bubbly flow, then got flattened in slug flow and tended to reach a steady value before transforming to annular flow.

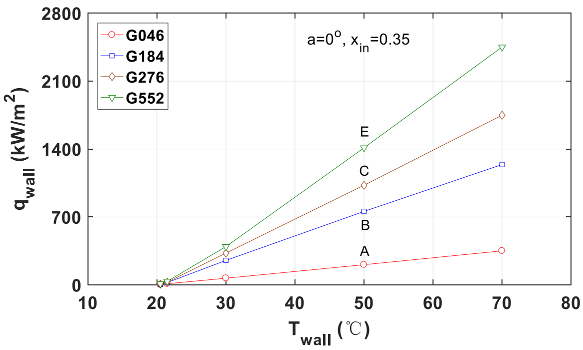

(a)

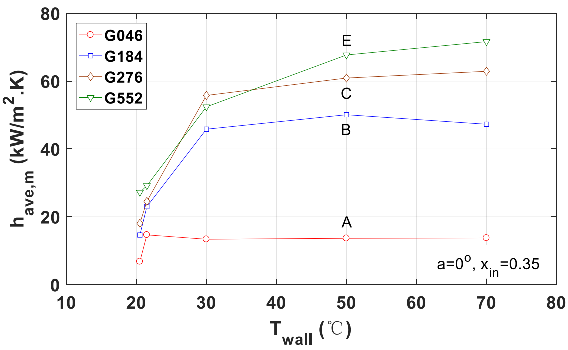

(b)

Fig. 13 The heating temperature effect on overall heat flux (a) and HTC (b) of NH_3/H_2O flow boiling in microchannel

3.3.2 The local heat transfer performance

The local heat flux and HTC at 276 kg/(m^2·s) are plotted based on different heating wall temperatures in Fig. 14. It can be observed from Fig. 14(a) that the local heat flux increased with heating wall temperature which is the driving force for NH_3/H_2O mixture flow boiling heat transfer. Whereas the slope of heat flux changing as a function of heating wall temperature was not the same for different locations at a1-a5. As shown in Fig. 14(a), the heat flux magnitude and the slope of heat flux vs. heating wall temperature decreased from a1 (red line) to a5 (blue line). This can be explained by that, as NH_3/H_2O flow boiling developed and NH_3 concentration in the bulk fluid decreased, it was nucleating boiling dominant bubbly flow at a1 near the microchannel inlet but approaching to convective dominant slug flow at a5 close to the outlet, as illustrated in Fig. 15(b). Furthermore, in Fig. 14(b), the HTC at T_{wall}=30 ˚C increased along the length of the microchannel (a1-a5) as the NH_3/H_2O mixture developed from subcooled flow boiling towards saturated flow boiling, as shown in Fig. 15(a). However, the HTC values at T_{wall}=50 ˚C and 70 ˚C were not considerably departed from each other except for HTC at location "a1" since the NH_3/H_2O mixture developed and reached to a certain stable flow boiling pattern faster at higher heating wall temperatures, as displayed in Fig. 15.

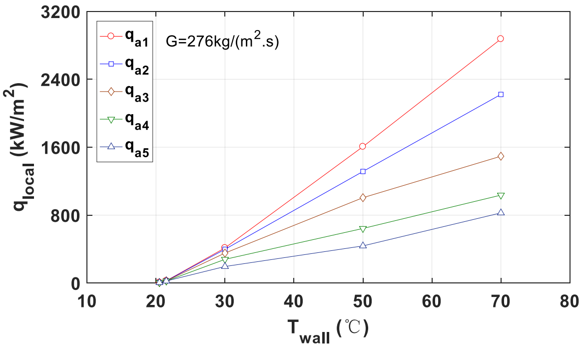

(a)

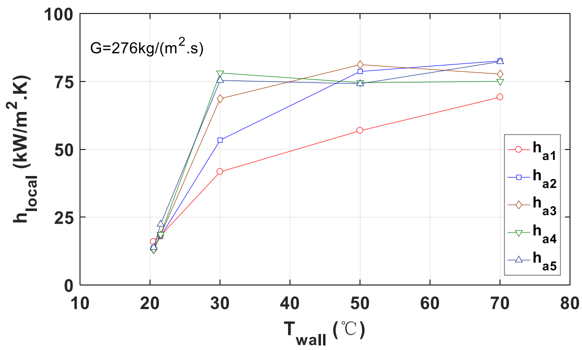

(b)

Fig. 14 The heating temperature effect on local heat flux (a) and HTC (b) at 276 kg/(m^2·s) of NH_3/H_2O flow boiling in microchannel

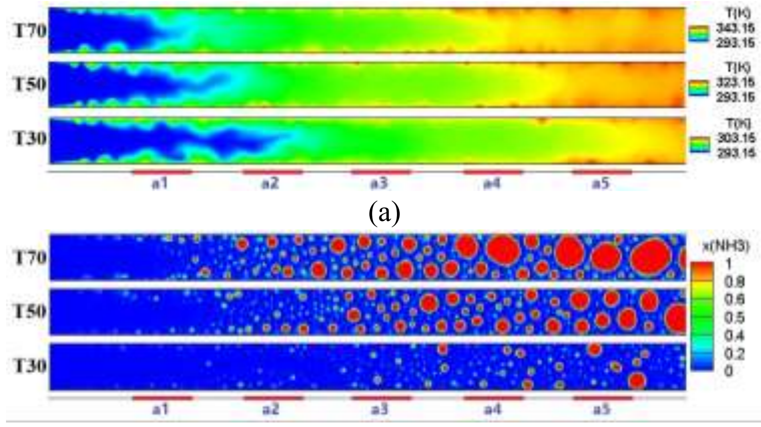

(a)

(b)

Fig. 15 The heating temperature effect on fluid temperature distribution (a) and vapor fraction distribution (b) of NH_3/H_2O flow boiling in microchannel

3.4 Overall performance evaluation of NH_3/H_2O flow boiling in the microchannel

The local HTC results of NH_3/H_2O flow boiling under various conditions of mass flow rate, inlet NH_3 concentration and heating wall temperature are summarized in Fig. 16(a) as a function of local wall vapor fraction, which is difficult to be physically and accurately measured in flow boiling experiments. As indicated in the figure, the numerical results of local HTC vs x_{wall}, regardless mass flow rate, inlet NH_3 concentration and heating wall temperature, followed the classic experimental M-shape curve of flow boiling HTC against local vapor quality, as shown in Fig. 16(b) for different types of working fluids [52-55]. It can be seen in Fig. 16(a), within the microchannel, the local HTC of NH_3/H_2O mixture linearly grew at low local wall vapor fraction (i.e. nucleation dominant region), declined in the middle (i.e. bubbly flow) after a maximum HTC value and kept decreasing with a slower rate at higher local wall vapor fractions (i.e. slug flow) until a sudden jump to a greater value (i.e. thin film evaporation flow) such as the "T70" curve. Furthermore, it can be concluded from the figure that flow boiling crisis and local dry-out were successfully prevented for NH_3/H_2O mixture under all the experimental conditions investigated in this study (i.e. $T_{wall} < 70$ ˚C, $x_{inlet} < 0.35$, $G < 552$ kg/(m^2·s)).

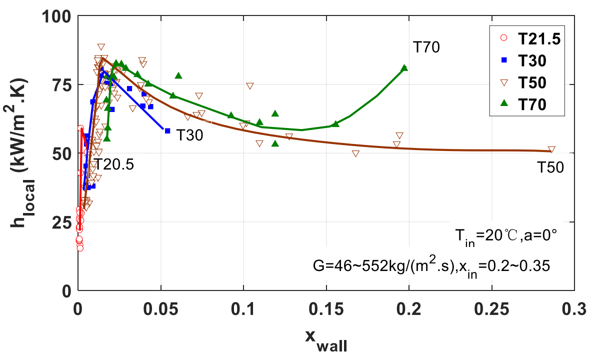

(a)

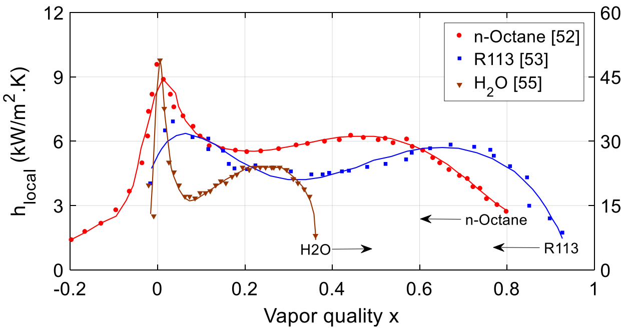

(b)

Fig. 16 Local HTC against vapor fraction on heating wall surface of NH_3/H_2O flow boiling in microchannel (a) present results (b) "M" shape curves in literature

4 Conclusions

In this study, numerical simulations were conducted to investigate the flow boiling heat transfer performance of NH_3/H_2O mixture in a single horizontal microchannel with 0.4 mm width and 6 mm length at various conditions. The effects of mass flux (46~552 kg/(m²·K)), inlet NH_3 concentration (0-35% by mole) and heating wall temperature (20.5~70 ˚C) on the overall and local heat transfer performance in the microchannel have been thoroughly evaluated. The main concluding remarks are as follows:

(1) Based on the numerical results, the flow boiling heat transfer performance of zeotropic NH_3/H_2O mixture in the microchannel was better than single-phase H_2O under a constant heating wall temperature of 50 ˚C. For the same mass flux of 552 kg/(m²·s), the heat dissipation rate of NH_3/H_2O mixture flow boiling could reach up to 1.41 MW/m², which was 2.05 times the value of H_2O single-phase convective cooling with 0.69 MW/m². While for achieving the same heat flux of 0.69 MW/m², the required mass flux of NH_3/H_2O flow boiling is 166.2 kg/(m²·s), which is 30% of the demanded H_2O flow for single-phase convective cooling.

(2) The numerical results showed that the NH_3/H_2O mixture flow boiling heat transfer in microchannel followed the general flow boiling characteristics except for the non-isothermal phase change feature of zeotropic NH_3/H_2O mixture (i.e. the saturation temperature of NH_3/H_2O mixture in the microchannel was a function of NH_3 concentration and pressure). The results also revealed that there was a threshold of inlet NH_3 concentration above which a steady level of heat dissipation rate was obtained at a given mass flow rate, that is, further increasing the inlet NH_3 concentration would no longer benefit the amount of heat being dissipated, for example, the threshold x_{in}=0.25 at G=184 kg/(m²·s).

(3) It was also indicated by the numerical simulations that the local HTC curve of NH_3/H_2O mixture flow boiling in the microchannel obeyed the general trend of the classic experimental M-shape curve of flow boiling HTC vs. local vapor quality. Furthermore, there were no local dry-outs throughout the microchannel length under all the simulation conditions in this study (i.e. $T_{wall} < 70$ ˚C, $x_{inlet} < 0.35$, G <

552 kg/(m^2·s)). Therefore, it can be concluded that the zeotropic NH_3/H_2O mixture is good at preventing local dry-outs and as a result it is a promising alternative coolant for maintaining a certain functional temperature of high power density electronic devices.

Declaration of conflicting interests

The authors declare that there is no conflict of interest.

Acknowledgement

The authors would like to acknowledge the financial support of the Engineering and Physical Sciences Research Council (EPSRC) of the United Kingdom (Grant Nos. EP/N000714/1 and EP/N021142/1).

Nomenclature

A	area (m^2)
E	energy (J/kg)
$\vec{F}_{surf}$	surface tension force (N/m^3)
h	Heat transfer coefficient ($kW/(m^2 \cdot K)$)
k_{eff}	effective thermal conductivity ($W/(m \cdot K)$)
p	pressure (Pa)
q_{LH}	Latent heat (J/kg)
q	Heat flux (kW/m^2)
r_i	relaxation factor during phase change process (m^{-1})
S_m	mass source term ($kg/(m^3 \cdot s)$)
S_h	energy source term ($J/(m^3 \cdot s)$)
T	temperature (K)
$T_{backflow}$	mass-averaged back-flow temperature (K)
u_x	velocity in the x direction at each grid cell (m/s)
$\vec{v}$	velocity (m/s)
x	NH_3 concentration in liquid NH_3/H_2O mixture (by mol)
y	NH_3 concentration in gaseous NH_3/H_2O mixture (by mol)

Greek symbols

α	volume fraction
κ	local interface curvature (m^{-1})
μ	dynamic viscosity ($kg/(m \cdot s)$)
ρ	density (kg/m^3)
σ	surface tension coefficient (N/m)

Subscripts

p, q	liquid and gas phases of fluid
sat	saturation
local	local heat transfer performance
overall	overall heat transfer performance
wall	heating wall

L, R	left and right side of heating wall
l, r	left and right side of heating wall
fluid	fluid parameter

References

[1] S.T. Kadam, R. Kumar, Twenty first century cooling solution: Microchannel heat sinks, Int. J. Therm. Sci. 85 (2014) 73-92.

[2] J.L. Wang, L. Zhao, and X.D. Wang, A comparative study of pure and zeotropic mixtures in low-temperature solar Rankine cycle, Appl. Energ. 87 (2010) 3366-3373.

[3] N. Zheng, J.J. Wei, L. Zhao, Analysis of a solar Rankine cycle powered refrigerator with zeotropic mixtures, Sol. Energy 162 (2018) 57-66.

[4] J.B. Marcinichen, J.A. Olivier, N. Lamaison, J.R. Thome, Advances in electronics cooling, Heat Transfer Eng. 34(5-6) (2013) 434-446.

[5] H.L.S.L Leão, F.J. do Nascimento, G. Ribatski, Flow boiling heat transfer of R407C in a microchannels based heat spreader, Exp. Therm. Fluid Sci. 59 (2014) 140-151.

[6] C. Guo, J. Wang, X. Du, L. Yang, Experimental flow boiling characteristics of R134a/R245fa mixture inside smooth horizontal tube, Appl. Therm. Eng. 103 (2016) 901-908.

[7] C. Dang, L. Jia, X. Zhang, Q. Huang, M. Xu, Experimental investigation on flow boiling characteristics of zeotropic binary mixtures (R134a/R245fa) in a rectangular micro-channel, Int. J. Heat Mass Transfer 115 (2017) 782-794.

[8] C. Dang, L. Jia, Q. Peng, L.F. Yin, Z.L. Qi, Experimental study on flow boiling heat transfer for pure and zeotropic refrigerants in multi-microchannels with segmented configurations, Int. J. Heat Mass Transfer 127 (2018) 758-768.

[9] M. Azzolin, S. Bortolin, D.D. Col, Flow boiling heat transfer of a zeotropic binary mixture of new refrigerants inside a single microchannel, Int. J. Therm. Sci. 110 (2016) 83-95.

[10] S. In, S. Baek, L.Jin, S. Jeong, Flow boiling heat transfer of R123/R134a mixture in a microchannel, Exp. Therm. Fluid Sci. 99 (2018) 474-486.

[11] C.R. Kharangate, I. Mudawar, Review of computational studies on boiling and condensation, Int. J. Heat Mass Transfer 108 (2017) 1164-1196.

[12] ANSYS FLUENT Theory Guide, ANSYS Inc., Canonsburg, PA, 2009.

[13] R. Banerjee, Turbulent conjugate heat and mass transfer from the surface of a binary mixture of ethanol/iso-octane in a countercurrent stratified two-phase flow system, Int. J. Heat Mass Transfer 51.25-26 (2008) 5958-5974.

[14] J.Y. Zhang, J. Wen, S. Deng, J.J. Bao, L. Zhao, 2D numerical study on flow boiling of zeotropic mixture isobutane/pentane in internal countercurrent flow system, Appl. Therm. Eng. 114 (2017) 1247-1255.

[15] A.A.S. Lima, A.A.V. Ochoa, J.A.P. Da Costa, J.R. Henriquez, CFD simulation of heat and mass transfer in an absorber that uses the pair ammonia/water as a working fluid, Int. J. Refrig. 98 (2019) 514-525.

[16] M.R. Kærn, A. Modi, J.K. Jensen, J.G. Andreasen, An assessment of in-tube flow boiling correlations for ammonia–water mixtures and their influence on heat exchanger size, Appl. Therm. Eng. 93 (2016) 623-

638.

[17] T. Khir, R.K. Jassim, N. Ghaffour, A.B. Brahim, Experimental study on forced convective boiling of ammonia-water mixtures in a vertical smooth tube, Arab.J. Sci. Eng. 30(1B) (2005) 47-63.

[18] M.P. Mishra, H.K. Varma, C.P. Sharma, Heat transfer coefficients in forced convection evaporation of refrigerants mixtures, Lett.in Heat and Mass Transfer 8(2) (1981) 127-136.

[19] F. Táboas, M. Valles, M. Bourouis, A. Coronas, Flow boiling heat transfer of ammonia/water mixture in a plate heat exchanger, Int. J. Refrig. 33 (2010) 695-705.

[20] F. Taboas, M. Valles, M. Bourouis, A. Coronas, Assessment of boiling heat transfer and pressure drop correlations of ammonia/water mixture in a plate heat exchanger, Int. J. Refrig. 35 (2012) 633-644.

[21] H. Arima, J.H. Kim, A. Okamoto, Y. Ikegami, Local boiling heat transfer characteristics of ammonia in a vertical plate evaporator, Int. J. Refrig. 33 (2010) 359-370.

[22] H. Arima, A. Okamoto, Y. Ikegami, Local boiling heat transfer characteristics of ammonia/water binary mixture in a vertical plate evaporator, Int. J. Refrig. 34 (2011) 648-657.

[23] D.M. van de Bor, C. Vasilescu, C.I. Ferreira, Experimental investigation of heat transfer and pressure drop characteristics of ammonia–water in a mini-channel annulus, Exp. Therm. Fluid Sci. 61 (2015) 177-186.

[24] S. Szczukiewicz, M. Magnini, J.R. Thome, Proposed models, ongoing experiments, and latest numerical simulations of microchannel two-phase flow boiling, Int. J. Multiphase Flow 59 (2014) 84-101.

[25] J. Lee, L.E. O'Neill, S. Lee, I. Mudawar, Experimental and computational investigation on two-phase flow and heat transfer of highly subcooled flow boiling in vertical upflow, Int. J. Heat Mass Transfer 136 (2019) 1199-1216.

[26] J. Patek, J. Klomfar, Simple functions for fast calculations of selected thermodynamic properties of the ammonia-water system. Int. J. Refrig. 18(4) (1995) 228-234.

[27] M. Conde-Petit, Thermodynamic properties of NH_3+H_2O mixtures for the industrial design of absorption refrigeration equipment, Zurich, Switzerland, 2006.

[28] C.B. Tibiriçá, G. Ribatski, Flow patterns and bubble departure fundamental characteristics during flow boiling in microscale channels, Exp. Therm. Fluid Sci. 59 (2014) 152-165.

[29] Z. Yang, X. F. Peng, P. Ye, Numerical and experimental investigation of two phase flow during boiling in a coiled tube, Int. J. Heat Mass Transfer 51 (2008) 1003-1016.

[30] R. Banerjee, K.M. Isaac, Evaluation of turbulence closure schemes for stratified two phase flow, in: 2003 ASME International Mechanical Engineering Congress and Exposition, Washington, DC, 2003.

[31] R. Revellin, V. Dupont, T. Ursenbacher, J.R. Thome, I. Zun, Characterization of diabatic two-phase flows in microchannels: Flow parameter results for R-134a in a 0.5 mm channel, Int. J. Multiphase Flow 32 (2006) 755-774.

[32] J.U. Brackbill, D.B. Kothe, C. Zemach, A continuum method for modeling surface tension, J. Comput.

Phys. 100 (1992) 335-354.

[33] W.H. Lee, A Pressure Iteration Scheme for Two-Phase Flow Modeling, Multiphase Transport Fundamentals, Reactor Safety, Applications, Hemisphere Publishing, Washington D.C., 1980.

[34] L. Yang, W. Li, J.Z. Zhang, W.J. Minkowycz. Analysis of thermal performance and pressure loss of subcooled flow boiling in manifold microchannel heat sink. Int. J. Heat Mass Transfer 162 (2020): 120362.

[35] L. Yang, J.Z. Zhang, W. Li. A comparative numerical study on two-phase boiling fluid flow and heat transfer in the microchannel heat sink with different manifold arrangements. Int. J. Heat Mass Transfer 156 (2020): 119864.

[36] C. Fang, M. David, A. Rogacs, K. Goodson, Volume of fluid simulation of boiling two-phase flow in a vapor venting microchannel, Front. Heat Mass Transfer 1(2010) 013002.

[37] K.C. Wong, J.H. Chong, Hydrodynamics and heat transfer prior to onset of nucleate boiling in a rectangular microchannel heat sink, Int. Commun. Heat Mass. 64 (2015) 34-41.

[38] Y. Luo, J. Li, K. Zhou, J. Zhang, W. Li, A numerical study of subcooled flow boiling in a manifold microchannel heat sink with varying inlet-to-outlet width ratio, Int. J. Heat Mass Transfer 139 (2019) 554-563.

[39] J. Kim, J.Y. Cho, J.S. Lee, Flow boiling enhancement by bubble mobility on heterogeneous wetting surface in microchannel, Int. J. Heat Mass Transfer 153 (2020) 1-13.

[40] N. Cheng, Y. Guo, C.H. Peng, A numerical simulation of single bubble growth in subcooled boiling water, Ann. Nucl. Energy 124 (2019) 179-186.

[41] Q. Liu, W. Wang, B. Palm, A numerical study of the transition from slug to annular flow in micro-channel convective boiling, Appl. Therm. Eng. 112 (2017) 73-81.

[42] Y.K. Prajapati, M. Pathak, M.K. Khan, A comparative study of flow boiling heat transfer in three different configurations of microchannels, Int. J. Heat Mass Transfer 85 (2015) 711-722.

[43] W. Qu, I. Mudawar, Flow boiling heat transfer in two-phase microchannel heat sinks – I. Experimental investigation and assessment of correlation methods, Int. J. Heat Mass Transfer 46 (2003) 2755-2771

[44] D. Liu, P.S. Lee, S.V. Garimella, Prediction of the onset of nucleate boiling in microchannel flow, Int. J. Heat Mass Transfer 48 (2005) 5134-5149.

[45] E. Sobierska, R. Kulenovic, R. Mertz, Heat transfer mechanism and flow pattern during flow boiling of water in a vertical narrow channel-experimental results, Int. J. Therm. Sci. 46 (2007) 1172-1181.

[46] L. Yin, R. Xu, P. Jiang, H. Cai, L. Jia, Subcooled flow boiling of water in a large aspect ratio microchannel, Int. J. Heat Mass Transfer 112 (2017) 1081-1089.

[47] Dang, Chao, et al. Experimental investigation on flow boiling characteristics of zeotropic binary mixtures (R134a/R245fa) in a rectangular micro-channel. Int. J. Heat Mass Transfer 115 (2017): 782-794

[48] Lemmon, Eric W., Marcia L. Huber, and Mark O. McLinden. NIST standard reference database 23. Reference fluid thermodynamic and transport properties (REFPROP), version 9.1 (2010).

[49] B. Yang, P. Wang, A. Bar-Cohen, Mini-contact enhanced thermoelectric cooling of hot spots in high power devices, IEEE Trans. Compon. Packag. Technol. 30 (3) (2007) 432-438.

[50] K. Zhou, C. Coyle, J. Li, J. Buongiorno, W. Li, Flow boiling in vertical narrow microchannels of different surface wettability characteristics, Int. J. Heat Mass Transf. 109 (2017) 103–114.

[51] W. Li, K. Zhou, J. Li, Z. Feng, H. Zhu, Effects of heat flux, mass flux and twophase inlet quality on flow boiling in a vertical superhydrophilic microchannel, Int. J. Heat Mass Transfer 119 (2018) 601–613.

[52] M. Cortina-Diaz, J. Schmidt, Flow boiling heat transfer of n-hexane and n-octane in a minichannel. In: Proceedings of the 13th International Heat Transfer Conference, Sydney, Australia, 2006.

[53] Y. Yang, Y. Fujita, Flow Boiling Heat Transfer and Flow Pattern in Rectangular Channel of Mini-Gap, in: ASME. International Conference on Nanochannels, Microchannels, and Minichannels, ASME 2nd International Conference on Microchannels and Minichannels. (2004) 573-580

[54] A. Bar-Cohen, E. Rahim, Modeling and prediction of two-phase microgap channel heat transfer characteristics, Heat Transfer Eng. 30 (8) (2009) 601-625

[55] K. Balasubramanian, M. Jagirdar, P.S. Lee, C.J. Teo, S.K. Chou, Experimental investigation of flow boiling heat transfer and instabilities in straight microchannels. Int. J. Heat Mass Transfer 66 (2013) 655-671.